Genetic characteristics of polycistronic system-mediated randomly-inserted multi-transgenes in miniature pigs and mice

SIYUAN KONG[1,2], LI LI[1], WENJUAN ZHU[1], LEILEI XIN[1], JINXUE RUAN[1], YUBO ZHANG[2], SHULIN YANG[1] and KUI LI[1,2]

[1]State Key Laboratory of Animal Nutrition, Key Laboratory of Farm Animal Genetic Resource and Germplasm Innovation of Ministry of Agriculture, Institute of Animal Sciences, Chinese Academy of Agricultural Sciences, Beijing 100193; [2]Animal Functional Genomics Group, Agricultural Genomes Institute at Shenzhen, Chinese Academy of Agricultural Sciences, Shenzhen, Guangdong 518120, P.R. China

Received November 13, 2016; Accepted June 28, 2017

DOI: 10.3892/mmr.2017.7842

Abstract. Multi-transgenic technology is superior to single transgenic technology in biological and medical research. Multi-transgene insertion mediated by a polycistronic system is more effective for the integration of polygenes. The multi-transgene insertion patterns and manners of inheritance are not completely understood. Copy number quantification is one available approach for addressing this issue. The present study determined copy numbers in two multi-transgenic mice (K3 and L3) and two multi-transgenic miniature pigs (Z2 and Z3) using absolute quantitative polymerase chain reaction analysis. For the F0 generation, a given transgene was able to exhibit different copy number integration capacities in different individuals. For the F1 generation, the most notable characteristic was that the copy number proportions were different among pedigrees ($P<0.05$). The results of the present study demonstrated that transgenes within the same vector exhibited the same integration trend between the F0 and F1 generations. In conclusion, intraspecific consistency and intergenerational copy numbers were compared and the integration capacity of each specific transgene differed in multi-transgenic animals. In particular, the copy number of one transgene may not be used to represent other transgenes in polycistronic vector-mediated multi-transgenic organisms. Consequently, in multi-transgenic experimental animal disease model research or breeding, copy numbers provide an important reference. Therefore, each transgene in multi-transgenic animals must be separately screened to prevent large copy number differences, and inconsistent expression between transgenes and miscellaneous data, in subsequent research.

Correspondence to: Professor Shulin Yang, State Key Laboratory of Animal Nutrition, Key Laboratory of Farm Animal Genetic Resource and Germplasm Innovation of Ministry of Agriculture, Institute of Animal Sciences, Chinese Academy of Agricultural Sciences, 2 Yuanmingyuan West Road, Beijing 100193, P.R. China
E-mail: yangshulin@caas.cn

Key words: multi-transgene, miniature pig, mice, copy number, experimental animal disease model

Introduction

The prevalence of transgenic animals, including medical experimental animals and agricultural domestic animals, has increased following the development of transgenic crops (1). Transgenic technology is able to quickly introduce advantageous traits in distantly-related species, which may not be accomplished via traditional cross-breeding (2). In agricultural research, transgenic technology is developing rapidly, although there is a bottleneck in the extension of transgene husbandry (1). The exploitation of economically-important traits in addition to meat production, milk production and other directly food-associated traits has become a focus for reforming the association between genetically modified organisms and livestock production (3). Notably, medical research requires the establishment of a large number of animal models of human disease-associated pathologies (3). In previous years, researchers have used pioneering transgenic editing technologies to prepare animal models, including mice and rats, to transform and humanize their genetic features (3-9). However, pigs are genetically closer to humans compared with rodents, particularly in terms of anatomy, physiology, pathology and metabolic dynamics (10). Therefore, swine have great potential economic value in fundamental medical research. Although rodents cannot be adapted to perform tests directly, such as human heterogeneous organ transplantation, and drug development findings in rodents may be invalid, mouse model research is important for animal husbandry and medical assessment.

Over the past decade, transgenic livestock have been used to investigate human disease, employing models including Alzheimer's disease-associated amyloid precursor protein (APP) K670Nt/M671L transgenic pig models (3), polycystic kidney disease polycystin-2 transgenic miniature pig models (11) and autosomal dominant polycystic kidney disease Myc proto-oncogene transgenic pig models (12). Regarding the delivery of a transgene, or the application of genome editors to modify endogenous genes, these models may be

used to efficiently model a subset of desired traits, particularly when considering monogenic human diseases. However, it is difficult to produce desired traits by altering the expression of a single specific gene, particularly when considering polygenic diseases, including Alzheimer's disease, Cushing's syndrome and type II diabetes. Therefore, multi-transgenic animal models are required. Previous studies have demonstrated that in a polycistronic system (single vector mounting polygenes), a vector with multiple genes connected by 2A peptides (13) may be more effective and efficient for the random integration of polygenes into the animal genome (14). It is important to characterize multi-transgenic animal integration. Fortunately, exogenous gene copy numbers are one of the important factors affecting the level of expression and genetic stability (15,16). The transgene copy number indicates the number of genomic transgene copies (17). In a multi-transgenic organism, prior to breeding, it is important to determine the levels of integration and their associations in terms of whether the different copies of integrated genes are consistent (18). An accurate measurement of exogenous gene copy number is important for establishing a transgenic animal model, in addition to being a prerequisite for follow-up phenotype and gene function analyses (19).

The single standard curve-absolute method [with internal reference (representative of the genomic copy number)] is an efficient method for the detection of transgene copy numbers (7,20). Fluorescent quantitative polymerase chain reaction (qPCR) analysis is used to draw a $\log_a N$-ΔCq absolute quantification standard curve (N indicates the copy number; ΔCq represents the difference in the fluorescence threshold between the exogenous gene and the reference gene; and $\Delta Cq=Cq_{transgene}-Cq_{internal}$) (21). Therefore, copy number is primarily calculated according to the ΔCq of the sample.

The present study investigated the integrated copy number variations in two multi-transgenic mouse models (K3 and L3) and two multi-transgenic miniature pig models [Z2 (6) and Z3 (5)]. K3 is an 11β-hydroxysteroid dehydrogenase-1 (11β-HSD1)-C/EBP homologous protein (CHOP)-human islet amyloid polypeptide (hIAPP) multi-transgenic mouse; L3 is an 11β-HSD1-dominant-negative gastric inhibitory polypeptide receptor ($GIPR^{dn}$)-hIAPP multi-transgenic mouse; Z2 is a $GIPR^{dn}$-hIAPP transgenic miniature pig; and Z3 is an 11β-HSD1-CHOP-hIAPP transgenic miniature pig. All four animals were subjected to random insertion. The exogenous genes are important for adipogenesis (11β-HSD1) (9,22), insulinogenesis ($GIPR^{dn}$) (23,24) and cellular apoptosis [hIAPP (25), and CHOP (26)]. Previous studies have sought to use the coexpression of these genes to generate transgenic miniature pig models simulating human obesity or diabetes (5,6). The copy number of each gene in these multi-transgenic animals may provide valuable information to help construct more consistent genetic backgrounds of multi-transgenic pedigrees. Whether the features of these organisms are similar will be assessed based on the results of the present study.

Materials and methods

Multi-transgenic animals and insertion vectors. The multi-transgenic animals included two male and female multi-transgenic mice (K3 and L3; age, 7-8 weeks; weight, 18-22 g) and two male and female multi-transgenic miniature pigs (Z2 and Z3), which were supplied by the laboratory (Key Laboratory of Farm Animal Genetic Resource and Germplasm Innovation of the Ministry of Agriculture, Beijing, China) (27). Mice were housed at a temperature of 20-22˚C and relative humidity of 30-70%, under 12-h light/dark cycles with free access to food and water. Pigs were housed at a temperature of 15-25˚C, relative humidity of 30-70%, under 12-h light/dark cycles with free access to food and water. The animals received humane care, and the present study was performed in strict accordance with the recommendations outlined in the Guide for the Care and Use of Laboratory Animals (Institute of Animal Sciences, Chinese Academy of Agricultural Sciences, Beijing, China). All procedures involving animals were approved by the Animal Care and Use Committee of the Germplasm Resource Center for Chinese Experimental Miniature Pigs (permit no. ACGRCM 2013-035). All efforts were made to minimize suffering. The ear pieces of piglets were collected after birth with rapid operation.

The insertion in K3 was mediated by the pcDNA3.1-11β-HSD1-CHOP-2A-hIAPP vector, in which 11β-HSD1 was driven by the liver-specific promoter porcine apolipoprotein E promoter, and CHOP and hIAPP were linked to the 2A peptide and driven by the pancreas-specific promoter porcine insulin promoter (PIP) (5); the insertion in L3 was mediated by the pcDNA3.1-11β-HSD1-$GIPR^{dn}$-2A-hIAPP vector, which was the same as the vector for K3, except that $GIPR^{dn}$ replaced CHOP; the insertion in Z2 was mediated by the pGL3-$GIPR^{dn}$-2A-hIAPP vector, in which $GIPR^{dn}$ and hIAPP, linked to 2A, were driven by PIP (6); and the insertion in Z3 was mediated by the pcDNA3.1-11β- HSD1-CHOP-2A-hIAPP vector, as in K3 (Fig. 1) (5). The four multi-transgenic mice and miniature pig vectors are presented in Fig. 1, all of which are single-molecule polycistronic systems. These transgenic animals are models of human diabetes. K3 and L3 mice were generated via zygote microinjection (2). Oosperm was used for microinjection (vectors were directly injected into the pronucleus), which are able to produce a transgenic pure line. Z2 and Z3 miniature pigs were produced through somatic cell nuclear transfer (SCNT) (17). The mouse strain was C57BL/6J, and the miniature pig strain was Wuzhishan (28).

Re-identification of multi-transgenic animals. An efficient high-salt method was adopted to isolate genomic DNA. A total of 300 μl saturated NaCl solution was added to a completely lyzed 1.5-ml tissue sample (K3 and L3 mouse tail pieces; Z2 and Z3 pig ear pieces) using tissue lysis buffer (BioTeke Corporation, Beijing, China) with proteinase K (Thermo Fisher Scientific, Inc., Waltham, MA, USA) and incubated overnight, followed by centrifugation at 12,400 x g, for 25-30 min at 4˚C. The supernatant was transferred to a new centrifuge tube and 700 μl isopropanol was added, followed by mixing to form the flocculent DNA precipitate. The DNA concentrations were determined using an automatic UV spectrophotometer (Promega Corporation, Madison, WI, USA). The DNA quality was verified by 1% agarose gel electrophoresis. The gel was stained with 5X Gel Red (Generay Biotech Co., Ltd., Shanghai, China) and visualized using Gel Doc XR+ Gel Documentation system (Bio-Rad Laboratories, Inc., Hercules, CA, USA). Pairs of primers were designed

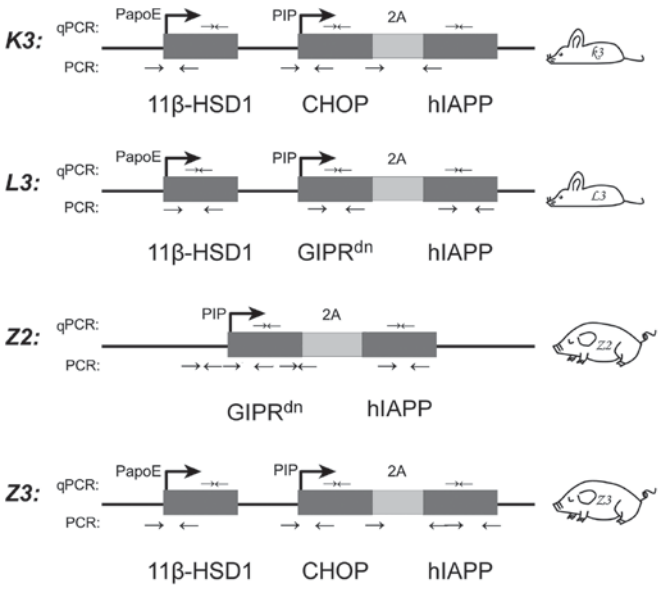

Figure 1. Schematic transgenic structure of the four multi-transgenic organisms. The arrows represent qPCR and PCR primer locations. PapoE, porcine apolipoprotein E promoter; PIP, porcine insulin promoter; 2A, 2A peptide; qPCR, quantitative polymerase chain reaction; 11β-HSD1, 11β-hydroxysteroid dehydrogenase-1; CHOP, C/EBP homologous protein; hIAPP, human islet amyloid polypeptide; $GIPR^{dn}$, dominant-negative gastric inhibitory polypeptide receptor.

using Primer Premier 5.0 (Premier Biosoft International, Palo Alto, CA, USA) for transgene fragments (Table I). The primers for K3 and Z3 were described in a previous study (5). Primer specificities were determined using Primer-BLAST (www.ncbi.nlm.nih.gov/tools/primer-blast). The exogenous genes were amplified via PCR (Beijing Eastwin Innovation Biotech Co., Ltd., Beijing, China), with the following components in each reaction (20 μl): 2 μl DNA template (500-1,000 ng/μl); 1 μl Primer F (10 μM); 1 μl Primer R (10 μM); 10 μl 2X Taq Mastermix (Takara Biotechnology Co., Ltd., Dalian, China); and 6 μl H_2O. The reaction parameters were as follows: 95˚C denaturation for 5 min; 30 cycles of 95˚C denaturation for 30 sec, annealing for 30 sec at the temperature stated in Table I, and 72˚C extension for 45 sec; followed by 72˚C extension for 10 min. The PCR products were evaluated via 1% agarose gel electrophoresis and stained with 5X Gel Red using a digital gel imaging system (Bio-Rad Laboratories, Inc.).

Development of gradient copy standard curves and determination of copy numbers. *Escherichia coli* DH5α competent cells (Takara Biotechnology Co., Ltd.) containing transgenic vector plasmids were incubated overnight on a shaker, and the plasmid DNA was extracted using an Endo-free Plasmid Mini kit (E.Z.N.A; Omega Bio-Tek, Inc., Norcross, GA, USA). K3 mice are described below as a representative example. The plasmid DNA concentration was measured (555 ng/μl). Positive identification of plasmid DNA was conducted by PCR, as aforementioned [Fig. 2; Z3 miniature pigs were verified positive in a previous study (5)]. Plasmid DNA was diluted by copy number gradient: 10^5; 10^4; 10^3; 10^2; 10; 1; and 0.1. Additionally, 100 ng (L3 mice, Z2 and Z3 miniature pigs: 10 ng) wild-type mouse DNA [extracted form mouse tail pieces of a C57BL/6 male mouse (age, 7-8 weeks; weight, 18-22 g) which was also housed at a temperature of 20-22˚C and relative humidity of 30-70%, under 12-h light/dark cycles with free access to food and water], was added to each gradient solution so that each solution system was more similar to the genomic DNA solution directly extracted from the transgenic individuals, thus homogenizing the reaction background (and introducing the wild-type reference gene). It was assumed that multi-exogenous gene fragments integrally inserted in the chromosome or transgene randomly as a whole unit in the forward or reverse orientation. The required vector mass was calculated using the following formula, which was adapted from (7):

$$\frac{\text{Transgenic plasmid vector mass}}{\text{Copy number} \times \text{transgenic plasmid vector length}} = \frac{\text{Wild-type mouse genomic mass}}{\text{Mouse haploid genomic DNA length} \times 2}$$

The total vector length was 13,525 bp, and the mouse haploid genome size was $3x10^9$ bp (7). According to the equation above, 10-fold gradient vector copy solutions were produced (Table II). Prior to the standard curve detection, solutions 1-7 were produced and 1 μl solutions A-G was added to each reaction system (Table II).

The exogenous gene copy number was determined via qPCR. The mouse haploid genome single-copy gene GAPDH was selected as an internal control for K3 and L3 (29,30). The porcine haploid genome single-copy gene transferrin receptor (TFRC) was selected as an internal control for Z2 and Z3 (16). The primer sequences are presented in Table I [except for K3 and Z3, which were described previously (5)]. qPCR was performed using the ABI 7500 Fast Real-Time PCR system (Applied Biosystems; Thermo Fisher Scientific, Inc.) and the SYBR® Premix Ex Taq™ kit (Takara Biotechnology Co., Ltd.) was used to generate the absolute quantification standard curve. The 20-μl qPCR reactions consisted of the following: 10 μl SYBR® Premix Ex Taq GC (2X); PCR forward primer (10 μM), 0.4 μl; PCR reverse primer (10 μM) 0.4 μl; ROX Reference Dye II (50X), 0.4 μl; template DNA 2.0 μl; ddH_2O, 6.8 μl. The experiment was repeated three times, and the results were averaged. The two-step PCR amplification procedure consisted of the following: Stage 1, initial denaturation of 95˚C for 30 sec; stage 2, 40 cycles of 95˚C for 10 sec and 60˚C for 30 sec. ΔCq-LgN standard curves (the targeted gene copy number logarithm corresponding to ΔCq; 11β-HSD1: K3 or L3 a=10, Z3 a=2; CHOP, hIAPP and $GIPR^{dn}$ a=10; outliers were eliminated) were generated using GraphPad Prism 5.0 (GraphPad Software, Inc., La Jolla, CA, USA). DNA samples of 100 ng (L3 mice, Z2 and Z3 miniature pigs: 10 ng) were used. The ΔCq for each gene was quantified based on the difference in fluorescence ($\Delta Cq=Cq_{transgene}-Cq_{internal}$), which may be calculated based on the standard curve to obtain the copy number.

Statistical analysis. One-way analysis of variance followed by a post hoc Duncan's new multiple range test was used to determine numerical differences in transgene copy numbers between different pedigrees to assess gene and individual integration capacity and diversity, using SPSS version 22.0 (IBM Corp., Armonk, NY, USA). ΔCq-LgN standard curves and graphs were drawn using GraphPad Prism version 6.01.

Table I. Primer sequences for the amplification and copy number quantification of exogenous genes.

Primer name	Primer sequence, 5'-3'	Ta, ˚C	Product, bp	Organism
Amplification				
11βHSD1-F	GTTCTGGAGGAGTGGGC	58	1,085	L3 multi-transgenic mice
11βHSD1-R	TAGGAAAGGACAGTGGGAG			
GIPR^{dn}-F	CAGGAGCAAGTGACCAGGAG	58	862	L3 multi-transgenic mice
GIPR^{dn}-R	GAGCAGGTAGTAGCGGAAGTG			
hIAPP-F	CTTCCTCAGCTCCTTCCA	58	910	L3 multi-transgenic mice
hIAPP-R	CTCCGCTCCATCGTTCA			
PIP-F	CGATGTTGGGCAAAGTATGA	58	424	Z2 multi-transgenic miniature pigs
PIP-R	GGTCTTGACGGATGAGTAGGA			
PIP-GIPR^{dn}-F	CTCAGGCCGCTCGTTAAGAC	58	952	Z2 multi-transgenic miniature pigs
PIP-GIPR^{dn}-R	GAGACAGGGAGTAGCCGACAGT			
GIPR$^{dn'}$-F	CATCAACAAGGAGGTGCAGTCG	58	265	Z2 multi-transgenic miniature pigs
GIPR$^{dn'}$-R	CAGCAGGTCGAAGTTCAGGGT			
hIAPP'-F	CCATTTGGTGGATTATACGGA	58	899	Z2 multi-transgenic miniature pigs
hIAPP'-R	TGTTATCATGTCTGCTCGAAG			
Copy number quantification				
11β-HSD1-F	GGCTCCCTGAATCCTACTC	60	167	L3 multi-transgenic mice
11β-HSD1-R	TCTTTCCTCGAAGCATCTC			
hIAPP-F	AGCTACACCCATTGAAAGTC	60	100	L3 multi-transgenic mice and Z2 multi-transgenic miniature pigs
hIAPP-R	GTTGCTGGAATGAACTAAAA			
GIPR^{dn}-F	TGTCGGCTACTCCCTGTC	60	144	L3 multi-transgenic mice and Z2 multi-transgenic miniature pigs
GIPR^{dn}-R	CGGTCTCGGCTGAGAATG			
GAPDH-F	AGGGCATCCTGGGCTACACT	60	166	K3 and L3 multi-transgenic mice
GAPDH-R	TCCACCACCCTGTTGCTGTAG			
TFRC-F	GAGACAGAAACTTTCGAAGC	60	81	Z2 and Z3 multi-transgenic miniature pigs
TFRC-R	GAAGTCTGTGGTATCCAATCC			

The primers for identification and copy number analysis for transgenes 11βHSD1, C/EBP homologous protein, hIAPP and reference genes in K3 mice and Z3 miniature pigs have been described in (5). Ta, annealing temperature; F, forward primer; R, reverse primer; PIP, porcine insulin promoter; bp, base pairs; 11β-HSD1, 11β-hydroxysteroid dehydrogenase-1; hIAPP, human islet amyloid polypeptide; GIPR^{dn}, dominant-negative gastric inhibitory polypeptide receptor; TFRC, transferrin receptor.

The dissociation curves were generated with ABI7500 SDS system software version 1.4.1 (Applied Biosystems, Thermo Fisher Scientific, Inc.). $P<0.05$ was considered to indicate a statistically significant difference.

Results

Re-identification of multi-transgenic mice and miniature pigs. A total of two multi-transgenic mice and two multi-transgenic miniature pigs were generated via random insertion of polycistronic vectors (Fig. 1). DNA samples were isolated from the F0 and F1 generations. The DNA (260/280 nm) absorbance ratios ranged from 1.8 to 2.0, which indicated that the DNA purity was optimal. PCR analysis using genomic DNA was used to re-identify positive samples (Fig. 2), and Z3 was been described previously (5). DNA samples from the positive individuals were used to determine the copy numbers.

Transgene gradient copy number standard curves. A qPCR dissolution curve demonstrated the specificity of the three primer pairs (Fig. 3A). Unimodal dissolution curves indicated that the primer specificities were good and that the subsequent results were reliable. For the four multi-transgenic animals, every target gene was associated with one plasmid standard curve for the calculation (Fig. 3B).

Determination of multi-transgenic copy numbers. The F0 transgene (11β-HSD1, hIAPP, GIPR^{dn}, CHOP) copy numbers of the four multi-transgenic animals (K3 and L3 mice; and Z2 and Z3 swine) are listed in Table III. In the F0 generation, for all transgenic genes, the copy numbers of the genes directly reflected the integrated situations of the four polycistronic systems. It was observed that the copy numbers of three genes (11β-HSD1, hIAPP, CHOP) in K3 mice were <90 (maximum copy number of all three genes=44.51;

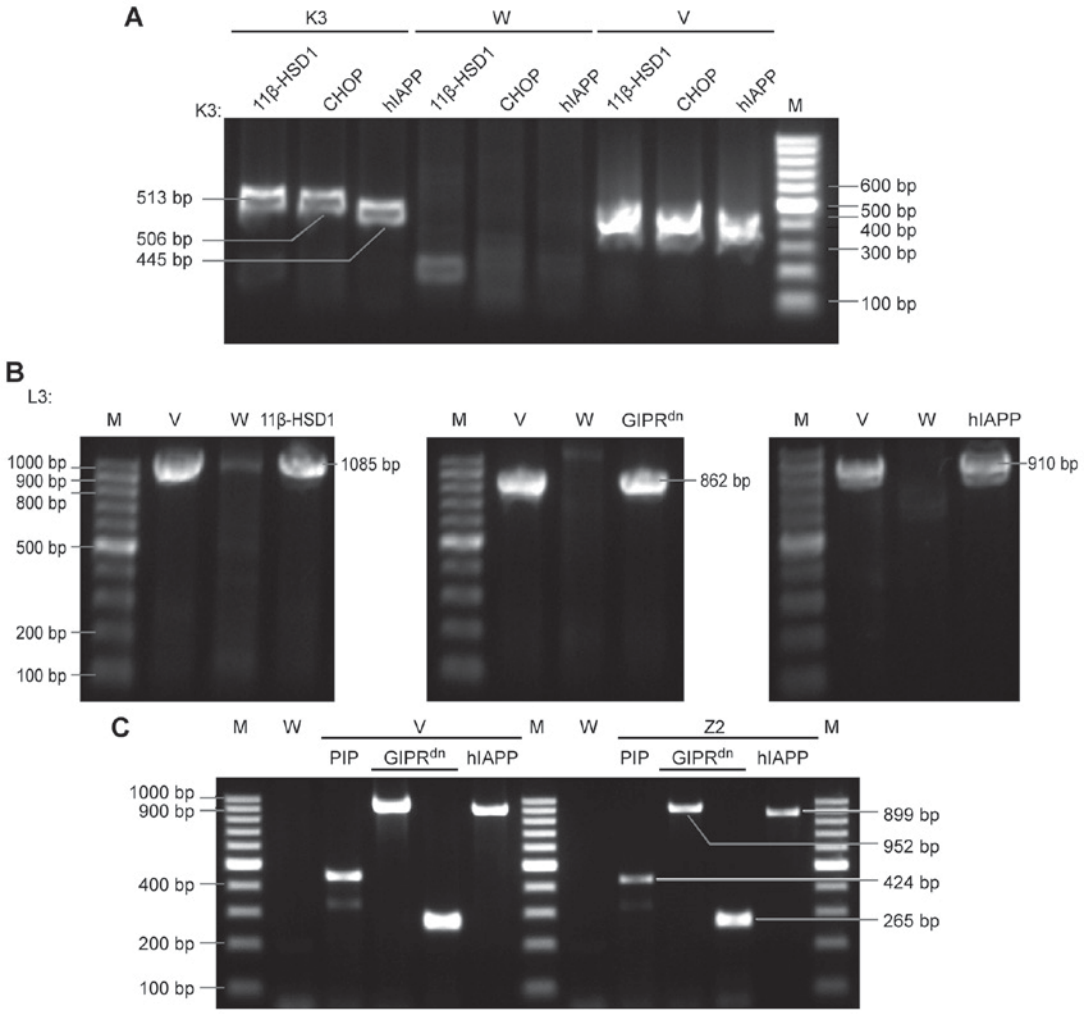

Figure 2. PCR re-identification electrophoretogram. (A) PCR analysis of triple transgenic K3 mice. Three lanes/individual, with the following main fragment order: 11β-HSD1, CHOP, and hIAPP. A total of three simultaneous bands was regarded as a positive result. (B) PCR analysis of triple transgenic L3 mice. Three exogenous main gene fragments were detected individually. (C) PCR analysis of dual transgenic Z2 miniature pigs. Four simultaneous bands were regarded as positive. The primers are listed in Table I. Marker, 100 bp DNA ladder. M, marker; V, positive control plasmid vector; W, negative control wild-type mice; 11β-HSD1, 11β-hydroxysteroid dehydrogenase-1; CHOP, C/EBP homologous protein; hIAPP, human islet amyloid polypeptide; GIPR^{dn}, dominant-negative gastric inhibitory polypeptide receptor; PIP, porcine insulin promoter; PCR, polymerase chain reaction.

<90), indicated as K3<90. Additionally, the copy numbers of three genes (11β-HSD1, hIAPP, GIPR^{dn}) were >90 in L3 mice (minimum copy number of all three genes=94.19; >90) and <90 in Z3 miniature pigs (maximum copy number of all three genes=54.68; <90). In Z2 miniature pigs, the hIAPP copy number was <90, whereas the GIPR^{dn} copy number was >90 (Table III). It is of note that 90 is simply a default threshold that is easy to compare, without having a specific meaning. On the other hand, for single selected genes, the copy numbers of 11β-HSD1 (in K3, L3 and Z3 animals), hIAPP (in K3, L3, Z2 and Z3 animals), CHOP (in K3 and Z3 animals) and GIPR^{dn} (in L3 and Z2 animals) were not consistent among the various genomes (copies compared in the same column, Table III). In addition, the following average copy numbers were observed in K3 mice (Fig. 4): 11β-HSD1, 20.27; hIAPP, 4.13; and CHOP, 4.54. Among the copy numbers of all three genes, 11β-HSD1 accounted for the largest proportion (70%) (among the proportions of all transgene copies from the same multi-transgenic animal), while those of the other two genes were small (~15%; Fig. 4A). Taken together with the observed F1 generation copy numbers, the results of the present study indicated that the capacity of pcDNA3.1-11β-HSD1-CHOP-hIAPP to integrate into these mice was as follows: 11β-HSD1>CHOP≈hIAPP (Fig. 4A and C). Similarly, in L3 mice: 11β-HSD1, 207.61; GIPR^{dn}, 221.45; and hIAPP, 234.06. These results demonstrated that the three transgenes were present in approximately equal proportions (31, 35 and 33%), potentially due to the pcDNA3.1-11β-HSD1-GIPR^{dn}-hIAPP integration capacity in mice: 11β-HSD1≈GIPR^{dn}≈hIAPP (Fig. 4B). For Z2 miniature pigs: hIAPP, 70.57; and GIPR^{dn}, 117.10, and the two genes were also inconsistent (38%<62%; Fig. 5). For Z3 miniature pigs: 11β-HSD1, 11.13; hIAPP, 34.26; and CHOP, 50.41, demonstrating their inequality in Z3 pigs (5). This result may have been due to the integration capacity of pcDNA3.1-11β-HSD1-CHOP-hIAPP in miniature pigs (11β-HSD1<hIAPP<CHOP) compared with mice (11β-HSD1>CHOP≈hIAPP) (Fig. 6). No defined patterns were observed regarding multi-transgenic copy number integration. If these transgenes were replaced, or the host was changed, or even the structure of the polycistronic system (vector) was

Table II. Positive plasmid standard curve: Copy number gradient solutions.

Serial numbers	Copy numbers	Product, ng	Standard linear construction
1	10^5	22.54	Solution A (3 μl of 555 ng/μl vector solution mixed with 70.87 μl ddH_2O): 22.54 ng/μl
2	10^4	2.254	Solution B (10 μl A to dilute to 100 μl): 2.254 ng/μl
3	10^3	$2.254x10^{-1}$	Solution C (10 μl B to dilute to 100 μl): 0.2254 ng/μl
4	10^2	$2.254x10^{-2}$	Solution D (10 μl C to dilute to 100 μl): $2.254x10^{-2}$ ng/μl
5	10^1	$2.254x10^{-3}$	Solution E (10 μl D to dilute to 100 μl): $2.254x10^{-3}$ ng/μl
6	1	$2.254x10^{-4}$	Solution F (10 μl E to dilute to 100 μl): $2.254x10^{-4}$ ng/μl
7	0.1	$2.254x10^{-5}$	Solution G (10 μl F to dilute to 100 μl): $2.254x10^{-5}$ ng/μl

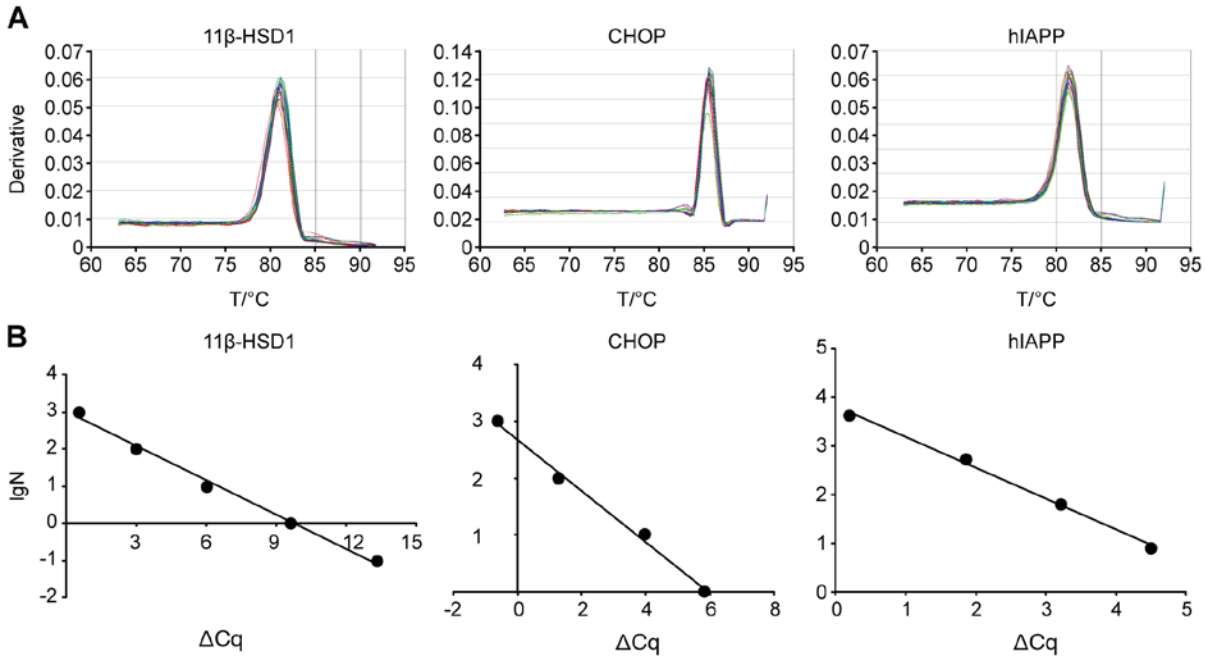

Figure 3. Representative dissociation curves and ΔCq-LgN standard curves. (A) Primer specificities of three exogenous primers for K3 11β-HSD1-hIAPP-CHOP multi-transgenic mice. (B) ΔCq-LgN standard curves of three transgenes. $\Delta Ct=Cq_{transgene}-Cq_{internal}$. 11βHSD1, y=-0.309x + 3.0101, R^2=0.9932; CHOP, y=-0.4509x + 2.6794, R^2=0.9947; and hIAPP, y=-0.6984x + 4.2135, R^2=0.996. L3 mice and Z2 and Z3 miniature pigs exhibited consistent results. 11β-HSD1, 11β-hydroxysteroid dehydrogenase-1; CHOP, C/EBP homologous protein; hIAPP, human islet amyloid polypeptide; T, temperature; lgN, decadic logarithm of the number of copies.

transformed, it may result in different copy numbers and insertion patterns. However, a single gene representing the overall integration was not feasible; i.e., one gene may not be representative of the integration capacities of other genes, even on the same vector.

F1 generation copies may reflect the integration status to some extent and may additionally reveal detailed differences among pedigrees, generations and organisms. The F1 generation was the descendant of a positive F0 male parent and several negative control female parents. The name of the F1 pedigree arises from the F0 male parental mark, excluding the Z2 miniature pigs from a negative female parental mark. Z2 miniature pig 4012 was the only positive F0 father. The copy numbers of exogenous genes in the F1 transgenic mice K3 and L3 and the transgenic miniature pigs Z2 and Z3 are presented in Table IV. The F1 integration trends of the different genes generally corresponded to the F0 male parents (Fig. 4A), excluding the L3 mice (Fig. 4B). L3 exhibited a copy number share of 11β-HSD1>GIPR^{dn}>hIAPP. However, L3 F0 was 11β-HSD1≈GIPR^{dn}≈hIAPP. Therefore, it was speculated that the copy number of 11β-HSD1 likely increased, which may directly influence the middle gene, GIPR^{dn}, due to their mostly collinear orientation in the genome (i.e., mediated by the same polycistronic vectors).

In order to identify intergenerational connections, the F0 and F1 generation copy numbers of multi-transgenic mice were compared (Fig. 4A and B). Although the L3 transgene copy number proportion was different between the F0 and F1 generations, the percentages of these genes in F1 pedigrees were approximately consistent (Fig. 4B and D). In K3 mice, the F1 copy numbers were equal to those in F0 (Fig. 4A), indicating that the three transgenes in K3 mice were likely a consequence of single locus integration. In L3 mice, the number of transgene copies was greater in F1 compared with

Table III. Copy numbers of exogenous genes for F0 transgenic mice (K3, L3) and transgenic miniature pigs (Z2, Z3).

Category	Number	11β-HSD1	hIAPP	GIPR^{dn}	CHOP
K3	6	44.51	11.62	n/a	8.31
K3	11	13.15	0.70	n/a	3.51
K3	12	3.15	0.08	n/a	1.80
K3	27	1.79	0.00	n/a	0.50
K3 average		20.27±10.17	4.13±3.06		4.54±1.59
L3	14	94.19	145.98	187.72	n/a
L3	18	192.97	175.06	197.69	n/a
L3	19	335.66	381.15	278.93	n/a
L3 average		207.61±57.23	234.06±60.44	221.45±23.58	
Z2	4012	n/a	70.57	117.10	n/a
Z3	1#	12.16	40.52	n/a	54.68
Z3	2#	10.09	28.01	n/a	46.13
Z3 average		11.13±0.73	34.26±4.42[a]		50.41±3.02[a]

K3, 11β-HSD1-CHOP-hIAPP multi-transgenic mouse; L3, 11β-HSD1-GIPR^{dn}-hIAPP multi-transgenic mouse; Z2, GIPR^{dn}-hIAPP transgenic pig; Z3, 11β-HSD1-CHOP -hIAPP transgenic pig. Number, ID number of animal. The numbers under each transgene refer to copy numbers, as determined by quantitative polymerase chain reaction analysis. One-way analysis of variance was used to determine significance. [a]P<0.05 vs. 11β-HSD1. 11β-HSD1, 11β-hydroxysteroid dehydrogenase-1; CHOP, C/EBP homologous protein; hIAPP, human islet amyloid polypeptide; GIPR^{dn}, dominant-negative gastric inhibitory polypeptide receptor.

F0 (Fig. 4B), particularly 11β-HSD1 (P<0.05; Table IV). The same phenomenon was observed in Z2 miniature pigs (GIPR^{dn}; Fig. 5C and D). In the F1 generation, the K3 inter-pedigree gene copy numbers were not consistent (Table IV). The multiple transgene copies in pedigrees 6 and 11 were greater than those in pedigrees 12 and 27 (Fig. 4C). The multi-transgenic percentages of the four pedigrees varied greatly in K3 (Table IV; Fig. 4C). Consequently, the F0 and F1 generations are sometimes not ideal for direct use as experimental subjects. The F2 or F3, or even subsequent generations, may be more suitable if the copy number is more consistent. Pie charts were generated to demonstrate the integration capacity in K3 mice (11β-HSD1>CHOP>hIAPP), which was concordant with the results obtained for the F0 generation (Fig. 4A and C). Specifically, in K3 pedigree 11, the hIAPP copy number was ~1; its vector likely fractured, resulting in decreased hIAPP insertion following integration. Additionally, the copies of hIAPP in pedigrees 12 and 27 were <0.2; thus, intact hIAPP may not have integrated in F0 12 and 27 K3 mice (Tables III and IV; Fig. 4C). However, the copy numbers of L3 mice were very large, and the transgene integration was more ordered than that in K3 mice (Fig. 4D). It is possible that the partial sequence fragment change impacted the characteristics of the entire vector. Additionally, Z2 miniature pigs (pGL3-GIPR^{dn}-hIAPP) were subjected to the distinguishing vector (Fig. 1), which carried only two transgenes, GIPR^{dn} and hIAPP (the two genes were the same as in L3). The present study obtained only one living F0 generation that was positive for Z2 (Fig. 2C). F0 was mated with 15 female wild-type miniature pigs, who delivered 41 transgenic, positive F1 piglets (Table IV). The transgene scatter was convergent (Fig. 5A). The copy number of GIPR^{dn} clearly exceeded that of hIAPP, and the vector may have fractured during integration. Connecting two points of the same pedigree (for example, 1086) demonstrated that the slopes among pedigrees were approximately equivalent (Fig. 5B). The copy numbers of the two genes, GIPR^{dn} and hIAPP, were altered almost proportionately as the F1 pedigrees resulted from only one positive male parent (Fig. 5B). The pie charts exhibited the percentages for the F0 male parent 4012, the average percentages for the F1 generation, and the percentages for specific individuals 10-86 and 11-61 (Fig. 5C). The proportions determined for the F1 generation were consistent (GIPR^{dn} ~20% vs. hIAPP ~80%), although the F0 percentage ratio was 40% vs. 60%. Therefore, in Z2 miniature pigs, transgenic integration was as follows: GIPR^{dn}>hIAPP, and the number of GIPR^{dn} copies increased between the F0 generation and the F1 generation. For Z3 triple-transgenic piglets, only two F0 individuals, 1# and 2#, were obtained (Fig. 6). The vectors used for the Z3 pigs were the same as those applied in the K3 mice (Fig. 1). Comparison of these two F0 individuals revealed that the integration capacity of the same vector was superior in Z3 pigs compared with K3 mice (Figs. 4A and 6; Table III). Additionally, transgene integration in Z3 was consistent among individuals (Fig. 6). Consequently, it was suggested that Z3 descendant F1 generations may serve directly as experimental subjects.

Discussion

The present study describes the analysis of multi-transgenic animals via qPCR based on the number of each integrated transgene. The premise upon which the present study was based is that to achieve regulated expression of multiple different transgenes in a single organism, large constructs containing all transgenes (either under the control of a specific promoter or linked by 2A-type sequences) are required, although such constructs may potentially fragment during the transgenesis process. Analysis of integrated transgenes is therefore required

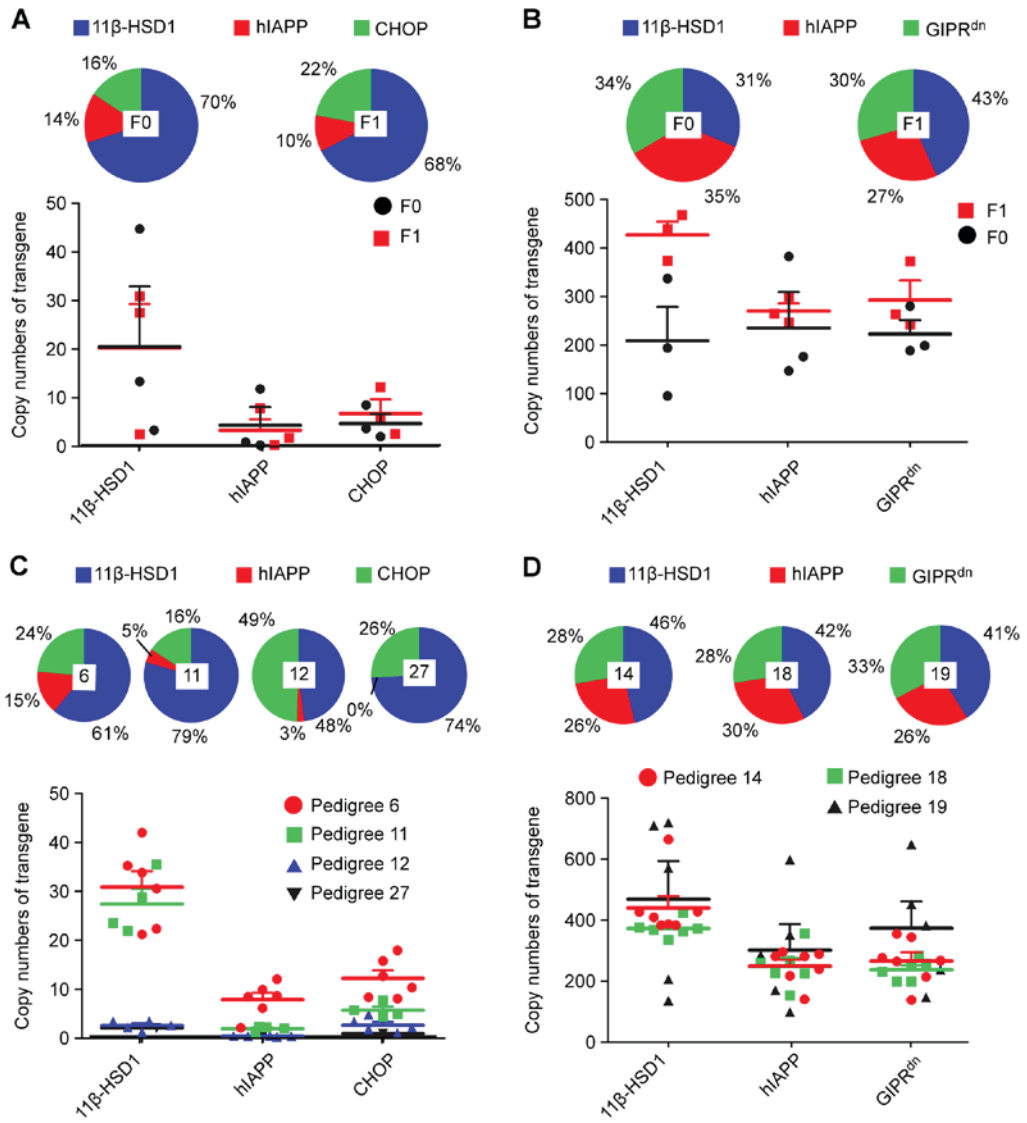

Figure 4. Copy number comparisons of transgenes in K3 and L3 mice. Copy number comparisons between the F0 and F1 generation from the perspectives of inter-individuals (scatter diagrams) and generational average copy numbers (pie charts) in (A) K3 mice and (B) L3 mice. Copy number comparisons of F1 generation transgenes in (C) K3 and (D) L3 mice from the perspectives of inter-pedigrees (scatter diagrams) and the proportions of individual exogenous genes in F1 (pie charts). 11β-HSD1, 11β-hydroxysteroid dehydrogenase-1; CHOP, C/EBP homologous protein; hIAPP, human islet amyloid polypeptide; $GIPR^{dn}$, dominant-negative gastric inhibitory polypeptide receptor.

(generally via qPCR) to understand potential future research or breeding strategies. In the present study, the methodology for the polycistronic vector systems was evaluated in diabetes-associated polygenic (11β-HSD11, hIAPP, CHOP and $GIPR^{dn}$) mice and miniature pigs, assuming that each construct integrated randomly as a whole unit into the genome. In the present study, real-time fluorescent single standard curve-absolute quantification (with an internal reference) was performed to determine the copy numbers in multi-transgenic animals (5,7,8,17,18,31). In a number of transgene copy number detection methods, a semi-quantitative technique is used, including traditional Southern blotting, and copy numbers are calculated through gray intensity analysis (4,32). As Southern blotting is time-consuming and semi-quantitative grey analysis may be inaccurate, this method may not be used alone to obtain an accurate copy number; other methods are required for confirmation. Absolute quantification methods can be broadly divided into a single standard curve (without an internal reference) quantification method, a single standard curve (with an internal reference) quantification method and a double standard curve ($Cq_{transgene}/Cq_{internal}$) quantification method. All these methods are based on qPCR. Since qPCR is quick and sensitive, it has been applied widely for copy number detection (33). The single standard curve (without an internal reference) method provides a positive gradient copy $\log_a N$-Cq absolute quantification standard curve (N indicates the copy number) (4). The sample copy numbers are subsequently calculated according to the Cq. The background solution of the standard curve system is pure water, although the transgenic sample background solutions are the genomic DNA solutions. Thus, the background solutions are inconsistent, and only approximate results may be obtained. The single standard curve (with an internal reference) method provides a positive gradient copy $\log_a N$-ΔCq absolute quantification standard curve. The difference in the fluorescence threshold, ΔCq, is substituted into the standard curve to derive the copy number

Table IV. Copy numbers of exogenous genes in F1 transgenic mice (K3, L3) and transgenic miniature pigs (Z2, Z3).

Category	Pedigree	Number	11β-HSD1	hIAPP	GIPR^{dn}	CHOP
K3	6	2	22.17	1.83	n/a	7.83
K3	6	6	30.42	11.81	n/a	15.56
K3	6	49	21.00	5.86	n/a	10.12
K3	6	55	35.14	9.64	n/a	17.74
K3	6	56	41.95	8.39	n/a	8.09
K3	6	58	33.74	8.17	n/a	12.46
Average	6		30.74±2.99	7.62±1.28[a]		11.97±1.51[a]
K3	11	9	35.45	1.89	n/a	5.42
K3	11	12	28.64	0.85	n/a	4.10
K3	11	46	21.71	1.72	n/a	4.68
K3	11	47	23.36	2.00	n/a	7.46
Average	11		27.29±2.68	1.615±0.23[a]		5.415±0.63[a]
K3	12	15	0.93	0.03	n/a	3.05
K3	12	16	3.15	0.16	n/a	0.75
K3	12	18	2.34	0.12	n/a	1.86
K3	12	23	1.87	0.18	n/a	1.55
K3	12	62	3.10	0.11	n/a	4.54
Average	12		2.28±0.37	0.12±0.02[a]		2.35±0.59
K3	27	27	1.79	0.01	n/a	0.62
Total average (K3)	6, 11, 12, 27		20.33±3.72	3.76±1.10[a]		7.13±1.41[a]
L3	14	5	383.90	284.93	351.76	n/a
L3	14	6	662.23	292.57	341.01	n/a
L3	14	48	406.19	277.63	261.24	n/a
L3	14	50	424.48	213.41	210.13	n/a
L3	14	51	423.92	277.34	263.53	n/a
L3	14	63	380.35	235.76	273.31	n/a
L3	14	68	380.12	136.24	134.58	n/a
Average	14		437.31±35.36	245.41±19.63[a]	262.22±26.09[a]	
L3	18	28	359.46	149.99	194.98	n/a
L3	18	41	332.14	223.24	195.22	n/a
L3	18	56	420.85	264.37	279.89	n/a
L3	18	84	369.04	257.04	250.97	n/a
L3	18	88	364.89	221.75	226.59	n/a
L3	18	91	372.92	352.40	253.03	n/a
Average	18		369.88±10.76	244.80±24.77[a]	233.45±12.73[a]	
L3	19	78	708.31	596.20	646.08	n/a
L3	19	81	568.38	282.64	379.75	n/a
L3	19	92	132.04	94.97	142.98	n/a
L3	19	94	717.64	349.28	449.98	n/a
L3	19	100	203.02	166.74	234.45	n/a
Average	19		465.88±111.93	297.97±77.52	370.65±78.13	
Total average (L3)	14, 18, 19		422.77±36.7	259.81±27.91[a]	282.75±30.55[a]	
Z2	11-9	2051	n/a	68.45	163.42	n/a
Z2	11-9	2053	n/a	47.22	147.47	n/a
Z2	10-86	2075	n/a	101.98	369.98	n/a
Z2	10-86	2078	n/a	35.16	154.85	n/a
Z2	10-86	2080	n/a	115.48	403.55	n/a
Z2	10-86	2081	n/a	126.82	473.91	n/a
Z2	10-86	2082	n/a	59.39	211.11	n/a
Z2	10-86	2083	n/a	104.10	355.35	n/a
Z2	11-61	2054	n/a	47.17	174.66	n/a
Z2	11-61	2056	n/a	56.48	210.23	n/a

Table IV. Continued.

Category	Pedigree	Number	11β-HSD1	hIAPP	GIPR^{dn}	CHOP
Z2	11-61	2059	n/a	71.71	396.92	n/a
Z2	156	2062	n/a	65.07	234.96	n/a
Z2	156	2064	n/a	63.27	195.52	n/a
Z2	11-15	2069	n/a	58.17	205.92	n/a
Z2	11-15	2071	n/a	63.01	284.71	n/a
Z2	11-15	2072	n/a	65.78	235.67	n/a
Z2	182	2138	n/a	57.16	154.17	n/a
Z2	132	2124	n/a	45.25	160.65	n/a
Z2	132	2126	n/a	52.01	157.65	n/a
Z2	132	2128	n/a	56.35	174.98	n/a
Z2	132	2129	n/a	77.34	178.44	n/a
Z2	10-83	2148	n/a	25.25	110.39	n/a
Z2	10-83	2149	n/a	80.98	151.69	n/a
Z2	8-12	2111	n/a	67.11	170.73	n/a
Z2	8-12	2113	n/a	0.37	0.45	n/a
Z2	8-12	2115	n/a	15.75	155.17	n/a
Z2	8-12	2116	n/a	15.72	170.84	n/a
Z2	8-12	2120	n/a	39.93	140.99	n/a
Z2	160	2144	n/a	67.48	191.21	n/a
Z2	160	2146	n/a	30.96	117.46	n/a
Z2	6-35	2132	n/a	30.23	132.43	n/a
Z2	6-35	2133	n/a	45.28	137.91	n/a
Z2	12-7	2139	n/a	42.10	79.43	n/a
Z2	12-7	2140	n/a	38.33	130.59	n/a
Z2	6-48	2152	n/a	38.22	131.22	n/a
Z2	6-48	2154	n/a	46.32	135.71	n/a
Z2	11-16	2155	n/a	49.79	149.55	n/a
Z2	164	2158	n/a	97.21	297.92	n/a
Z2	164	2159	n/a	41.00	112.77	n/a
Z2	164	2160	n/a	67.01	184.96	n/a
Z2	164	2162	n/a	42.13	155.77	n/a
Total average (Z2)	all Z2			56.55±4.07	192.71±14.47[b]	

K3, 11β-HSD1-CHOP-hIAPP multi-transgenic mouse; L3, 11β-HSD1-GIPR^{dn}-hIAPP multi-transgenic mouse; Z2, GIPR^{dn}-hIAPP transgenic pig. The F1 generation of Z3 was not obtained as F0 was sacrificed at a young age. One-way analysis of variance was used to assess significance. [a]P<0.05 vs. 11β-HSD1; [b]P<0.05 vs. hIAPP; 11β-HSD1, 11β-hydroxysteroid dehydrogenase-1; CHOP, C/EBP homologous protein; hIAPP, human islet amyloid polypeptide; GIPR^{dn}, dominant-negative gastric inhibitory polypeptide receptor.

directly (5,7,8,31). The common point of these two methods is sufficient to draw a standard curve for a particular gene, and they differ because the former considers only the exogenous gene fluorescence threshold, Cq, as an independent variable, while the latter considers the difference, ΔCq, between the exogenous gene and the reference gene as the independent variable. Since the reference gene represents the background -the wild-type genome- the latter copy numbers are corrected according to the wild-type control for improved accuracy. This correction step is one of the reasons why the present method was adopted. Additionally, in the double standard curve ($Cq_{transgene}/Cq_{internal}$) method for the target gene and reference gene, two known copy gradient standard curves are established using qPCR, which provides simultaneous quantitative detection of the exogenous and reference genes. The copy numbers of the exogenous and reference genes in the sample are subsequently determined; the number of copies of the exogenous gene in the haploid genome is the ratio of the copy number of the exogenous gene to that of the internal reference gene (34). Here, we note that ΔCq and $Cq_{transgene}/Cq_{internal}$ represent a reference gene correction strategy. One is corrected in the reaction system (by relative quantitation of the control reaction system error by benchmarking the fluorescence threshold of the reference gene), and the other is corrected by copy number mathematical correction (thus ΔCq is optimal). In addition, $Cq_{transgene}/Cq_{internal}$ requires the construction of two standard lines with error reduplicates. In addition, the relative quantification ($2^{-\Delta\Delta Cq}$) method, which completely

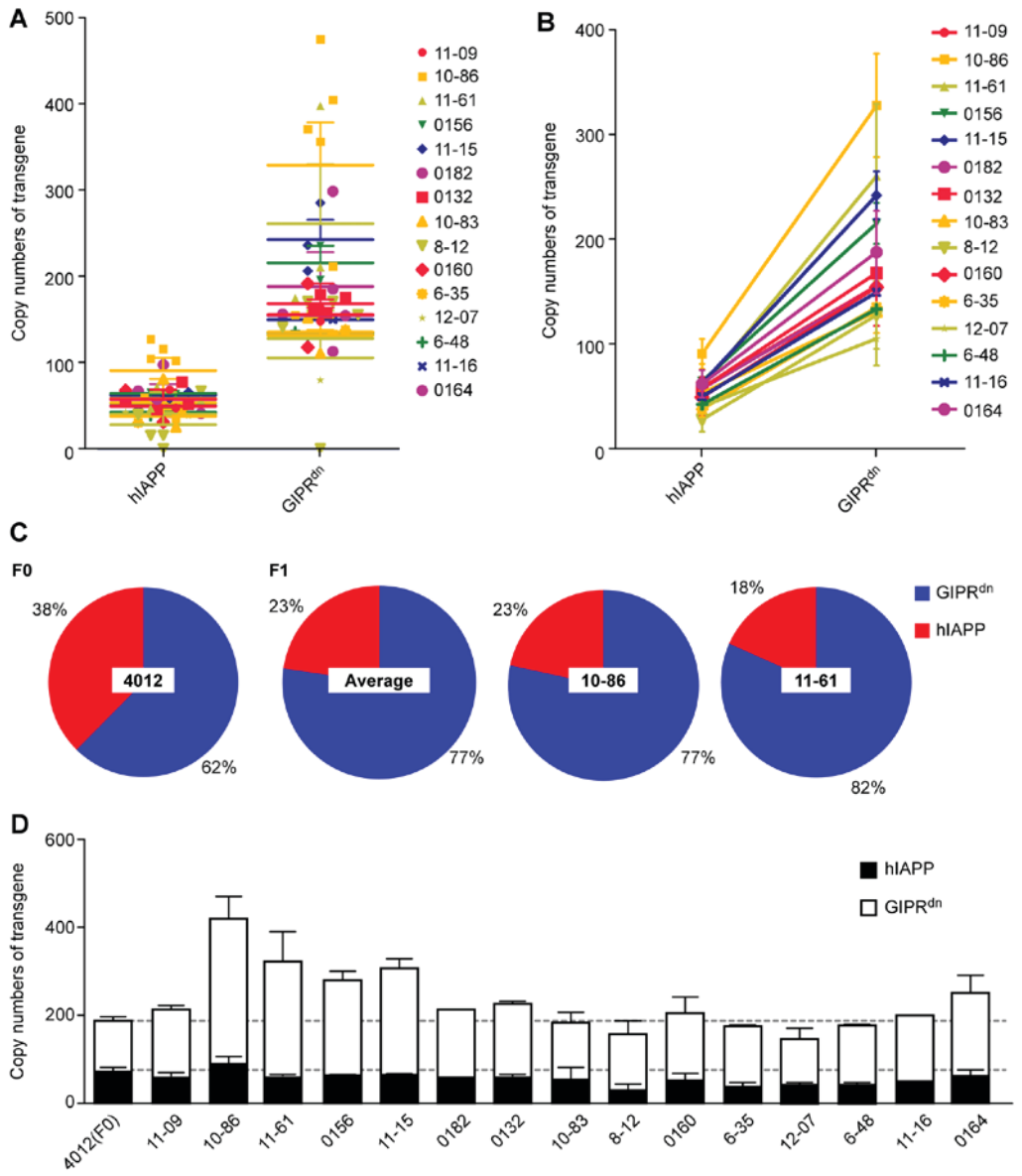

Figure 5. Copy numbers characteristic of dual-transgenic hIAPP and GIPR^{dn} in Z2 miniature pigs. Z2 represents GIPR^{dn}-hIAPP transgenic miniature pigs. The personal identification numbers were derived from the female parents (wild-type control). (A) Convergence degree of the two exogenous gene copy plots, comprising all F1 offspring. (B) The results in different angles of the slope line, exhibiting the degree of integrity of the integration of the two genes. (C) Copy number proportions in the Z2 miniature pig father F0 and representative F1 individuals. (D) Copy number comparison of transgenes in Z2 miniature pigs between F0 and F1 individuals. hIAPP, human islet amyloid polypeptide; GIPR^{dn}, dominant-negative gastric inhibitory polypeptide receptor.

adopts the idea of relative quantitation of expression, is also based on algorithm correction (35). Specifically, the negative control group genomic DNA is mixed with an equal copy number of positive plasmid solution as a reference sample. The reference gene is used to adjust the system error (also ΔCq). The transgenic sample ΔCq and the reference sample ΔCq are then compared ($2^{-\Delta\Delta Cq}$), where $2^{-\Delta\Delta Cq}$ represents the number of transgene copies inserted (18). Since this method is based on logarithms, the reaction trends of the data are very reliable, although their digital accuracy is less consistent. The relative quantification ($2^{-\Delta\Delta Cq}$) method requires a more stringent internal gene copy (must be 1), and the error is larger. Comparison of these methods revealed that the single standard curve-absolute quantification method (with an internal reference) is ideal for determining the copy number in transgenic pigs and mice (5,7,8,31).

The copy numbers of randomly integrated transgenes in multi-transgenic mice and miniature pigs were determined. In the present study, the quantitative dissociation curves were unimodal, confirming the specificity of the primers (15,35,36). In the development of the gradient copy standard curve, it was assumed that PCR efficiency is generally equal between a plasmid template and genomic DNA (7,8,31). The statistical results indicated that the pedigree copy numbers in K3 F1 mice were significantly different. For the same exogenous gene, the copy numbers in F1 mice from different founder (F0) generations varied widely. Therefore, the F1 with the ideal, consistent copy number was able to be selected for future research (deleting the individuals with failure of multi-gene integration). The screening policy ought not to focus solely on high copy numbers. It has been reported that high transgene copy numbers may result in co-suppression between genes, mainly

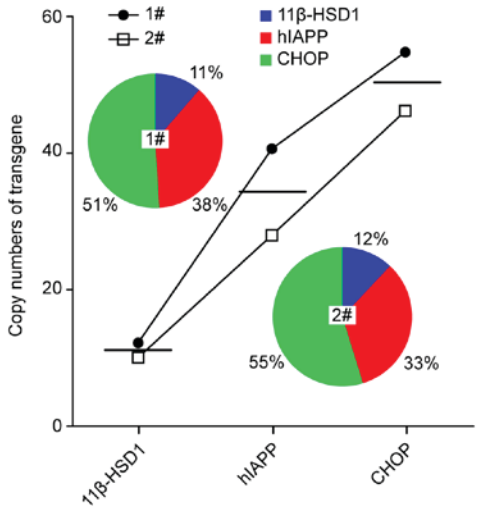

Figure 6. Transgene copy numbers in Z3 miniature pigs. Z3 represents the 11β-HSD1-CHOP-hIAPP transgenic pig. The broken line graph indicates the average value between F0 piglets 1# and 2#. The pie charts exhibit the proportions of the three transgene copy numbers. 11β-hydroxysteroid dehydrogenase-1; CHOP, C/EBP homologous protein; hIAPP, human islet amyloid polypeptide.

due to transcriptional or post-transcriptional silencing (37,38). It is necessary to eliminate individuals carrying multi-genes that are not integrated or individuals with very low transgene copy numbers. However, the positive individuals with either two or three gene copies exhibited a lack of regularity in terms of integration numbers. In addition, the copy number in the offspring (F1) with an F0 parent exhibiting a high transgene copy number was high, particularly in L3. However, the copy number of integrated hIAPP was lower in K3 mice, providing a value of zero in several pedigrees (12,27). Three-gene integrations of hIAPP in K3 and L3 were both low. In Z2 miniature pigs, hIAPP integration was also decreased compared with $GIPR^{dn}$ (Fig. 5), suggesting that the integration of hIAPP is more difficult. However, in Z3 miniature pigs, the hIAPP copy number was not the lowest (Fig. 6). Therefore, it may involve numerous biological factors (including homology of the transgene to the host). However, it is of note that considering integrated sites and late phenotypes (including western blotting or certain later research data) are also important factors in selecting ideal multi-transgenic animals; copy number is only one of the factors.

In polycistronic random integration series in multi-transgenic animals, each gene integrates inconsistently in the genome, resulting in the comparison of genetically modified animals with multiple differences. The transgene preparation vectors are too large for these animals. The integration of a series of multiple genes, and particularly the occurrence of different levels of fracture during the integration process, may result in the integration of different gene-associated sequences of various lengths (39). For example, in Z2 F0 miniature pigs, transgenic copies were $GIPR^{dn}$>hIAPP, indicating that certain events may have occurred, including fragmentation. Zhang *et al* (39) used whole genome sequencing to assay transgenic cattle, which adopted a single transgene; they observed that certain transgene fragments were indeed fragmented. Fragmentation is an inherent shortcoming of polycistronic vector-mediated technology, but the observed data in other studies indicated that functional genes and even complete tandem gene structures were present (5,6,14,17). However, the copy number qPCR detection method from the present study was widely used. Specifically, if fracturing of large constructs during the transgenesis process is as significant a factor as indicated by the analysis performed in the present study, quantifying parts of each integrated transgene via qPCR may not be satisfactory, as it will not demonstrate the entirety of the transgene. Additionally, if fracturing is indeed such a problem for large transgenes, then large transgenes are unlikely to be a tenable platform for the reliable production of multi-transgenic animals. However, a number of copies or incomplete fragments of transgenes are likely to be integrated into different sites of the genome, in the manner of a shotgun blast hitting an object, increasing the difficulty and uncertainty associated with the accurate detection of these gene copies (39). Nevertheless, qPCR remains an important method for measuring the copy numbers of transgenes (7,8), as numerous transgenic genes are incomplete in the single-transgene genomes (39). In addition, the multi-transgenic Z2 and Z3 miniature pigs and multi-transgenic K3 and L3 mice (mouse data awaiting publication) used in the present study exhibited the expected phenotypes to a certain degree (5,6). Deng *et al* (14) combined the 2A peptide and double promoters to efficiently mediate the co-expression of the four fluorescent proteins in pigs, and the present study therefore considered this to be a promising methodology for generating multi-transgenic pigs via a single nuclear transfer. Tian *et al* (13) generated 2A peptide-mediated tri-fluorescent protein gene-expressing transgenic sheep. Park *et al* (17) successfully generated transgenic pigs expressing soluble human tumor necrosis factor receptor superfamily member 1A Fc fusion protein and human heme oxygenase 1 using the F2A peptide, which demonstrated that utilization of the F2A self-cleaving peptide polycistronic system is a promising tool for generating multi-transgenic pigs. The results of the present study further demonstrated the existence of inconsistent copy numbers following random integration associated with multiple genes loaded in a single carrier. Thus, the copy number of one transgene may not be used to represent the copy numbers of other co-loaded transgenes. As expected, it was observed that polycistronic-mediated transgenes integrate as large fragments, and it is difficult to determine the integrity of all integrated gene sequences. Additionally, it remains questionable whether this phenomenon is also due to the presence of promoters (which may facilitate easier fragmentation) from heterogeneous sources in these animals. If the carrier only contains sequences from homologous species, different results (different forms of fragmentation) may be obtained, potentially resulting in more consistent multiple gene copy numbers. However, to answer these questions, further research is required.

The detection principle of the method used in the present study is derived from the average number of transgene copies in the haploid genome. It was proposed that if F0 transgenic events primarily occur in the same homologous chromosome, then future generations will not comply with the copy number halved law, and the F0 and F1 transgene copy numbers may be equal (individuals with negative copy detection were eliminated

from the results of the present study presented in Tables III and IV). The transgene copy number of one of the transgenes in L3 mice and Z2 pigs increased relative to the other two transgenes during germline transmission (F0 to F1). F0 multi-transgenesis randomly inserted in mouse 40 chromosomes or porcine 38 chromosomes. When meiosis occurs, the transgenes will separate irregularly. It is possible that homologous recombination between sister chromatin is one of the reasons why there may be a difference in the F1 generation. The negative control parent may influence the genomic background and thus lead copy number half-and-half alterations mathematically. Certain gametes exhibit high copy (even more than 2-fold) transgene, after mate with the negative, some F1 still more than F1 average transgene copy number level. However, homologous gametes would exhibit low copy numbers. In addition, non-sister chromatid exchange may weaken the influence of the negative control parent (as a way to reduce the F1 difference). Similarly, non-sister chromatid exchange may be the single reason (as a way to enlarge the F1 difference), since the proportions determined for the F1 generation were consistent ($GIPR^{dn}$ ~20% vs. hIAPP ~80%), although the F0 percentage ratio was 40% vs. 60%. qPCR analysis has been widely used in copy number detection, although the limitation was that it used a pair of primers, following amplification, which reflected the copy number by fragment length 80-150 bp (the general product length of qPCR), and is therefore not very accurate. The copy numbers in the present study may reflect only a general value or trend. More accurate copy number detection may be obtained with the help of whole genome resequencing (39). Additionally, certain other rare causes may be implicated. An increasing copy number may be responsible for copy number variation regions, which are similar to the integration of exogenous fragments since as-yet-unclear events may occur during such a random integration (40). For example, whether restructuring exists, similar to the formation of the genetic structure of an antibody (41), non-allelic homologous recombination occurs during meiosis, which will generate repetitive copy variation and structural rearrangements between sequences (42). DNA damage, like non-homologous end-joining, may not be fully restored, or replication forks may be stalled, generating copies of repeated sequence (43). Transposon jumping, followed by their insertion at active hot spots, may additionally cause copy generation and genomic instability (44,45).

Multi-gene copy detection, combined with other detection methods, including site junction and later transgenic expression, to direct selection will avoid intra-treatment differences and indistinct phenotype data in subsequent experiments. Copy detection is one of the important aspects for transgene assessments, biosafety assessments and inspection applications. In fact, reliance solely on qPCR results in difficulties associated with accurate assessments of gene integrity, integration sites and the precise number of integrated gene copies. Notably, whole genome sequencing may be a good tool to improve the effectiveness of transgene integration detection (39). In order to completely elucidate integration characteristics in multi-transgenic animals, researchers may focus on site-targeting or copy-targeting of future transgenes to avoid the various subsequent uncertainties [the RNA-guided CRISPR Cas9 system (46) allows site-specific integration]. The present study used miniature pigs produced via somatic cell nuclear transfer to measure copy numbers. However, all of the analyses may be performed in donor cells, rather than in live animals, which may decrease the cost.

In conclusion, the results of the present study indicated that the integration capacities of different polycistronic system-mediated vectors vary in different multi-transgenic mice and miniature pigs, and the integration of each gene via different vectors in different genomes is inconsistent. In addition, although two or three genes were loaded by the same vector, their integrated copy numbers were not concordant, even in different genomes. The copy number of one gene may not be used to represent that of other genes in the same transgenic organism. In animal experiments utilizing random multi-transgene incorporation, copy number is one of the most important factors for consideration; if transgenic mice are directly adopted for research following manufacture without selection and future breeding, numerous differences and miscellaneous data will emerge in subsequent research.

Acknowledgements

The present study was supported by the National Natural Science Foundation of China (grant no. 31372276), the State Key Laboratory of Animal Nutrition (grant no. 2004DA125184G1602), the National Basic Research Program of China (grant no. 2015CB943100), the Agricultural Science and Technology Innovation Program (grant nos. ASTIP-IAS05 and ASTIP-IAS-TS-4), and Shenzhen Special Fund for the Strategic Emerging Industries Development (grant no. CXZZ20140504105105077).

References

1. Tizard M, Hallerman E, Fahrenkrug S, Newell-McGloughlin M, Gibson J, de Loos F, Wagner S, Laible G, Han JY, D'Occio M, *et al*: Strategies to enable the adoption of animal biotechnology to sustainably improve global food safety and security. Transgenic Res 25: 575-595, 2016.
2. Miao X: Recent advances in the development of new transgenic animal technology. Cell Mol Life Sci 70: 815-828, 2013.
3. Fan N and Lai L: Genetically modified pig models for human diseases. J Genet Genomics 40: 67-73, 2013.
4. Gao S, Yang Y, Wang C, Guo J, Zhou D, Wu Q, Su Y, Xu L and Que Y: Transgenic sugarcane with a cry1Ac gene exhibited better phenotypic traits and enhanced resistance against sugarcane borer. PLoS One 11: e0153929, 2016.
5. Kong S, Ruan J, Xin L, Fan J, Xia J, Liu Z, Mu Y, Yang S and Li K: Multi-transgenic minipig models exhibiting potential for hepatic insulin resistance and pancreatic apoptosis. Mol Med Rep 13: 669-680, 2016.
6. Kong S, Ruan J, Xin L, Fan J, Zhu W, Xia J, Li L, Yang S and Li K: Type 2 diabetes model of minipig generated by multi-gene transgenic technology. Diabetes Metab Res Rev 31: 26, 2015.
7. Luo W, Li Z, Huang Y, Han Y, Yao C, Duan X, Ouyang H and Li L: Generation of AQP2-Cre transgenic mini-pigs specifically expressing Cre recombinase in kidney collecting duct cells. Transgenic Res 23: 365-375, 2014.
8. Luo W, Li Z, Li P, Huang Y, Han Y, Yao C, Zhang Z, Yan H, Pang D, Ouyang H and Li L: Expression of Cre recombinase in alveolar epithelial cells of the AQP2-Cre transgenic mini-pigs. Cell Physiol Biochem 34: 1597-1613, 2014.
9. Paterson JM, Morton NM, Fievet C, Kenyon CJ, Holmes MC, Staels B, Seckl JR and Mullins JJ: Metabolic syndrome without obesity: Hepatic overexpression of 11beta-hydroxysteroid dehydrogenase type 1 in transgenic mice. Proc Natl Acad Sci USA 101: 7088-7093, 2004.
10. Whyte JJ and Prather RS: Genetic modifications of pigs for medicine and agriculture. Mol Reprod Dev 78: 879-891, 2011.

11. He J, Ye J, Li Q, Feng Y, Bai X, Chen X, Wu C, Yu Z, Zhao Y, Hu X and Li N: Construction of a transgenic pig model overexpressing polycystic kidney disease 2 (PKD2) gene. Transgenic Res 22: 861-867, 2013.
12. Ye J, He J, Li Q, Feng Y, Bai X, Chen X, Zhao Y, Hu X, Yu Z and Li N: Generation of c-Myc transgenic pigs for autosomal dominant polycystic kidney disease. Transgenic Res 22: 1231-1239, 2013.
13. Tian Y, Li W, Wang L, Liu C, Lin J, Zhang X, Zhang N, He S, Huang J, Jia B and Liu M: Expression of 2A peptide mediated tri-fluorescent protein genes were regulated by epigenetics in transgenic sheep. Biochem Biophys Res Commun 434: 681-687, 2013.
14. Deng W, Yang D, Zhao B, Ouyang Z, Song J, Fan N, Liu Z, Zhao Y, Wu Q, Nashun B, *et al*: Use of the 2A peptide for generation of multi-transgenic pigs through a single round of nuclear transfer. PLoS One 6: e19986, 2011.
15. Zhu H, Wen F, Li P, Liu X, Cao J, Jiang M, Ming F and Chu Z: Validation of a reference gene (BdFIM) for quantifying transgene copy numbers in Brachypodium distachyon by real-time PCR. Appl Biochem Biotechnol 172: 3163-3175, 2014.
16. Kong QR, Wu ML, Zhu J, Bou G, Huan YJ, Yin Z, Mu YS and Liu ZH: Transgene copy number and integration site analysis in transgenic pig. Prog Biochem Biophys 12: 016, 2009.
17. Park SJ, Cho B, Koo OJ, Kim H, Kang JT, Hurh S, Kim SJ, Yeom HJ, Moon J, Lee EM, *et al*: Production and characterization of soluble human TNFRI-Fc and human HO-1 (HMOX1) transgenic pigs by using the F2A peptide. Transgenic Res 23: 407-419, 2014.
18. Qian X, Kraft J, Ni Y and Zhao FQ: Production of recombinant human proinsulin in the milk of transgenic mice. Sci Rep 4: 6465, 2014.
19. Webster NL, Forni M, Bacci ML, Giovannoni R, Razzini R, Fantinati P, Zannoni A, Fusetti L, Dalprà L, Bianco MR, *et al*: Multi-transgenic pigs expressing three fluorescent proteins produced with high efficiency by sperm mediated gene transfer. Mol Reprod Dev 72: 68-76, 2005.
20. Batista RI, Luciano MC, Teixeira DI, Freitas VJ, Melo LM, Andreeva LE, Serova IA and Serov OL: Methodological strategies for transgene copy number quantification in goats (Capra hircus) using real-time PCR. Biotechnol Prog 30: 1390-1400, 2014.
21. Song P, Cai C, Skokut M, Kosegi B and Petolino J: Quantitative real-time PCR as a screening tool for estimating transgene copy number in WHISKERS™-derived transgenic maize. Plant Cell Rep 20: 948-954, 2002.
22. Freude S, Heise T, Woerle HJ, Jungnik A, Rauch T, Hamilton B, Schölch C, Huang F and Graefe-Mody U: Safety, pharmacokinetics and pharmacodynamics of BI 135585, a selective 11β-hydroxysteroid dehydrogenase-1 HSD1 inhibitor in humans: Liver and adipose tissue 11β-HSD1 inhibition after acute and multiple administrations over 2 weeks. Diabetes Obes Metab 18: 483-490, 2016.
23. Campbell JE, Ussher JR, Mulvihill EE, Kolic J, Baggio LL, Cao X, Liu Y, Lamont BJ, Morii T, Streutker CJ, *et al*: TCF1 links GIPR signaling to the control of beta cell function and survival. Nat Med 22: 84-90, 2016.
24. Herbach N: Clinical and pathological characterization of a novel transgenic animal model of diabetes mellitus expressing a dominant negative glucose-dependent insulinotropic polypeptide receptor (GIPR dn). Ludwig Maximilians Universitat Munchen, Munich, Germany, 2002.
25. Matveyenko AV and Butler PC: Islet amyloid polypeptide (IAPP) transgenic rodents as models for type 2 diabetes. ILAR J 47: 225-233, 2006.
26. Eizirik DL, Cardozo AK and Cnop M: The role for endoplasmic reticulum stress in diabetes mellitus. Endocr Rev 29: 42-61, 2008.
27. Yang SL, Xia JH, Zhang YY, Fan JG, Wang H, Yuan J, Zhao ZZ, Pan Q, Mu YL, Xin LL, *et al*: Hyperinsulinemia shifted energy supply from glucose to ketone bodies in early nonalcoholic steatohepatitis from high-fat high-sucrose diet induced Bama minipigs. Sci Rep 5: 13980, 2015.
28. Fang X, Mou Y, Huang Z, Li Y, Han L, Zhang Y, Feng Y, Chen Y, Jiang X, Zhao W, *et al*: The sequence and analysis of a Chinese pig genome. GigaScience 1: 1-11, 2012.
29. Bustin SA: Absolute quantification of mRNA using real-time reverse transcription polymerase chain reaction assays. J Mol Endocrinol 25: 169-193, 2000.
30. Lin WS, Wang P, Cheng X, Yuan SL, Chen HX, Lin YL, Tao HX, Wang YC and Wang LC: Estimation of the copy numbers of exogenous gene in transgenic mice using the real-time fluorescence quantitative PCR based comparative Ct method. Lett Biotechnol 11: 301-305, 2013.
31. Li L, Li Q, Bao Y, Li J, Chen Z, Yu X, Zhao Y, Tian K and Li N: RNAi-based inhibition of porcine reproductive and respiratory syndrome virus replication in transgenic pigs. J Biotechnol 171: 17-24, 2014.
32. Armour JA, Sismani C, Patsalis PC and Cross G: Measurement of locus copy number by hybridisation with amplifiable probes. Nucleic Acids Res 28: 605-609, 2000.
33. D'haene B, Vandesompele J and Hellemans J: Accurate and objective copy number profiling using real-time quantitative PCR. Methods 50: 262-270, 2010.
34. Kai LI, Gao HL, Gao L, Xiaole QI, Gao YL, Yanwei XU and Wang XM: Development of a real-time PCR for determination of foreign gene copy number in genome of pichia pastoris. Chin J Anim Vet Sci 42: 742-746, 2011.
35. Yu L, Liu JP, Zhuang ZX, Yang LQ, Zhang RL, Ye XM and Cheng JQ: Quantitative analysis of real-time PCR expression production by REST and 2~((-ΔΔCT)). J Trop Med 10: 008, 2007.
36. Haurogné K, Bach JM and Lieubeau B: Easy and rapid method of zygosity determination in transgenic mice by SYBR Green real-time quantitative PCR with a simple data analysis. Transgenic Res 16: 127-131, 2007.
37. Tang W, Newton RJ and Weidner DA: Genetic transformation and gene silencing mediated by multiple copies of a transgene in eastern white pine. J Exp Bot 58: 545-554, 2007.
38. Vaucheret H and Fagard M: Transcriptional gene silencing in plants: Targets, inducers and regulators. Trends Genet 17: 29-35, 2001.
39. Zhang R, Yin Y, Zhang Y, Li K, Zhu H, Gong Q, Wang J, Hu X and Li N: Molecular characterization of transgene integration by next-generation sequencing in transgenic cattle. PLoS One 7: e50348, 2012.
40. Wu Y, Fan H, Jing S, Xia J, Chen Y, Zhang L, Gao X, Li J, Gao H and Ren H: A genome-wide scan for copy number variations using high-density single nucleotide polymorphism array in Simmental cattle. Anim Genet 46: 289-298, 2015.
41. Arrossi AV, Merzianu M, Farver C, Yuan C, Wang SH, Nakashima MO and Cotta CV: Nodular pulmonary light chain deposition disease: An entity associated with Sjögren syndrome or marginal zone lymphoma. J Clin Pathol 69: 490-496, 2016.
42. Tessereau C, Léoné M, Buisson M, Duret L, Sinilnikova OM and Mazoyer S: Occurrence of a non deleterious gene conversion event in the BRCA1 gene. Genes Chromosomes Cancer 54: 646-652, 2015.
43. Lachaud C, Moreno A, Marchesi F, Toth R, Blow JJ and Rouse J: Ubiquitinated Fancd2 recruits Fan1 to stalled replication forks to prevent genome instability. Science 351: 846-849, 2016.
44. Hastings PJ, Lupski JR, Rosenberg SM and Ira G: Mechanisms of change in gene copy number. Nat Rev Genet 10: 551-564, 2009.
45. Alessio AP, Fili AE, Garrels W, Forcato DO, Olmos Nicotra MF, Liaudat AC, Bevacqua RJ, Savy V, Hiriart MI, Talluri TR, *et al*: Establishment of cell-based transposon-mediated transgenesis in cattle. Theriogenology 85: 1297-1311, 2016.
46. Ruan J, Li H, Xu K, Wu T, Wei J, Zhou R, Liu Z, Mu Y, Yang S, Ouyang H, *et al*: Highly efficient CRISPR/Cas9-mediated transgene knockin at the H11 locus in pigs. Sci Rep 5: 14253, 2015.